

RESEARCH ARTICLE

WILEY

Threshold of vapour–pressure deficit constraint on light use efficiency varied with soil water content

Dexin Gao¹  | Shuai Wang¹ | Zidong Li¹ | Fangli Wei² | Peng Chen¹ | Shuang Song¹ | Yaping Wang¹ | Lixin Wang³ | Bojie Fu^{1,2}

¹State Key Laboratory of Earth Surface Processes and Resource Ecology, Faculty of Geographical Science, Beijing Normal University, Beijing, China

²State Key Laboratory of Urban and Regional Ecology, Research Center for Eco-Environmental Sciences, Chinese Academy of Sciences, Beijing, China

³Department of Earth Sciences, Indiana University–Purdue University Indianapolis (IUPUI), Indianapolis, Indiana, USA

Correspondence

Wang Shuai, Faculty of Geographical Science, Beijing Normal University, Beijing, 100875, China.
Email: shuaiwang@bnu.edu.cn

Funding information

Fundamental Research Funds for the Central Universities; National Natural Science Foundation of China, Grant/Award Numbers: 41991230, The Fundamental Research Funds for the Central Uni

Abstract

Understanding the constraints on light-use efficiency (*LUE*) induced by high evaporative water demand (vapour–pressure deficit; *VPD*) and soil water stress (soil moisture content; *SMC*) is crucial for understanding and simulating vegetation productivity, particularly in the arid and semi-arid regions. However, the relative impacts of *VPD* and *SMC* on *LUE* are unclear, as we lack a mechanistic understanding of impacts and their interactions. In this study, we quantified the relative roles of *VPD* and *SMC* in limiting *LUE* and analysed the interactions among *VPD*, *SMC* and *LUE* using data from CO_2 and water flux stations and weather stations along a climatic gradient in the Heihe River Basin, China. We found a threshold of *VPD* constraint on *LUE*; above the threshold, *LUE* decreased at only 3.6% to 23.1% of the rate below the threshold. As *SMC* decreased, however, the *VPD* threshold increased, and the reduction of *LUE* caused by *VPD* decreased significantly, which is more than half of that in moister regions. Therefore, both *VPD* and *SMC* played essential roles in *LUE* limitation caused by water stress. A threshold also existed for heat flux and the correlation between *SMC* and *LUE*; the strength of the correlation first decreased and then increased with increasing *VPD*. Our results clarified the relative impacts of *VPD* and *SMC* on *LUE*, and can improve simulation and prediction of plant productivity.

KEYWORDS

carbon simulation uncertainty, dryland, *LUE*, *SMC*, threshold, *VPD*

1 | INTRODUCTION

Atmospheric water demand, which is defined by the vapour–pressure deficit (*VPD*), and soil water supply (soil moisture content; *SMC*) together determine the level of plant water stress, and strongly affects photosynthesis. Light use efficiency (*LUE*), defined as the ratio of productivity and intercepted radiation (Monteith & Moss, 1977), tightly couples with plant transpiration and stomatal conductance (Novick et al., 2016). Stomatal conductance directly responds to rising *VPD* (Fletcher et al., 2007). High levels of *VPD* decrease stomatal conductance (Grossiord et al., 2020) and lead to reduction of *LUE* (Wu et al., 2013). *SMC* is the direct source of available water for plants to maintain photosynthesis (Trugman et al., 2018) and insufficient

SMC can decrease photosynthesis (Bartlett et al., 2016). Water stress can decrease the conductance of stem and stoma, resulting in significant decrease in photosynthesis (Mccarter & Price, 2014; Taylor et al., 2016). Overall, both *VPD* and *SMC* strongly affect plants *LUE* and carbon budget (Rigden et al., 2020). *VPD* and *SMC* change significantly over time in response to changes in temperature and precipitation (Stocker et al., 2013). *VPD* will significantly increase with rising temperatures (McDowell & Allen, 2015; Yuan et al., 2019). However, the response of *SMC* to climate change is uncertain, since some regions will experience increased precipitation and others will experience decreased precipitation (Stocker et al., 2013). The different trajectories of *VPD* and *SMC* require a better understanding of *VPD* and *SMC* controls on plant water stress under climate change. Thus,

studying the effects of *VPD* and *SMC* on *LUE* is necessary to support simulation and prediction of future plant productivity.

The relative importance of *VPD* and *SMC* in the regulation of photosynthesis remain unclear, leading to large uncertainty in productivity simulations (Stocker et al., 2019; Yuan et al., 2014). Some studies have found that increasing *VPD* can significantly decrease vegetation productivity by causing declines in carbon uptake and plant growth (Novick et al., 2016; Yuan et al., 2019). However, *SMC* constraint on *LUE* indicated that *SMC* was so important that would cause 40% reduction of *LUE* (Stocker et al., 2018). Effect of *SMC* on photosynthesis would further increase after decoupling *VPD* and *SMC*, whereas constraint of *VPD* decreased (Liu, Gudmundsson, et al., 2020). On the other hand, both *VPD* and *SMC* are essential for simulation of crop yield. Accounting for only *VPD* would lead to overestimate of the yield loss caused by water stress by a factor of two (Rigden et al., 2020).

Both *VPD* and *SMC* play important roles in plant water stress but through different mechanisms: *VPD* affects water demand whereas *SMC* affects water supply (Hsiao et al., 2019). Furthermore, there is inherent correlation between *VPD* and *SMC*, so the two factors interact to determine plant water status, which regulates *LUE* (Novick et al., 2016). Thus, disagreement over their relative importance may result from different perspectives on how *VPD* and *SMC* affect *LUE* and how *VPD* interacts with *SMC*. The relative magnitudes of the impacts of *SMC* and *VPD* on photosynthesis and the associated mechanisms remain unclear (Liu, Kumar, et al., 2020; Seneviratne et al., 2010). It is therefore necessary to study how *VPD* and *SMC* constrain *LUE*, particularly at a regional-scale. Accounting for these constraints in regional scale would decrease the uncertainty caused

by other factors, such as difference in N deposition and soil texture in different regions (Lanning et al., 2019).

To provide insights into these factors, we performed a study in the Heihe River Basin in China, where heat and CO_2 fluxes are measured and weather stations have been established along a climate gradient. This paper aims to understand the relative impacts of *VPD* and *SMC* on *LUE*, thereby providing an improved basis for simulating and predicting vegetation productivity. Specifically, we studied the interaction between *VPD*, *SMC* and *LUE* to clarify (1) the relative constraining effect of *VPD* and *SMC*, and (2) the process of constraining by *VPD* and *SMC*.

2 | METHODS

2.1 | Study area

The Heihe River Basin covers an 821-km length of rivers in an area of $1.429 \times 10^5 \text{ km}^2$, and it is the second largest inland river basin in China (Figure 1). There is strong climatic variation within the basin because of its large size. The mean annual precipitation (MAP) ranges from 36 to 444 mm and decreases from south to north. In the upper basin, which covers $1.001 \times 10^4 \text{ km}^2$, MAP is more than 350 mm. The middle reaches cover $3.388 \times 10^4 \text{ km}^2$, with MAP of 50 to 250 mm. In the lower reaches, however, MAP is <50 mm (Wang et al., 2019). In 2015, the HiWATER eco-hydrological observation network was set up in the basin to monitor eco-hydrological processes in the different climate zones (Song, 2019).

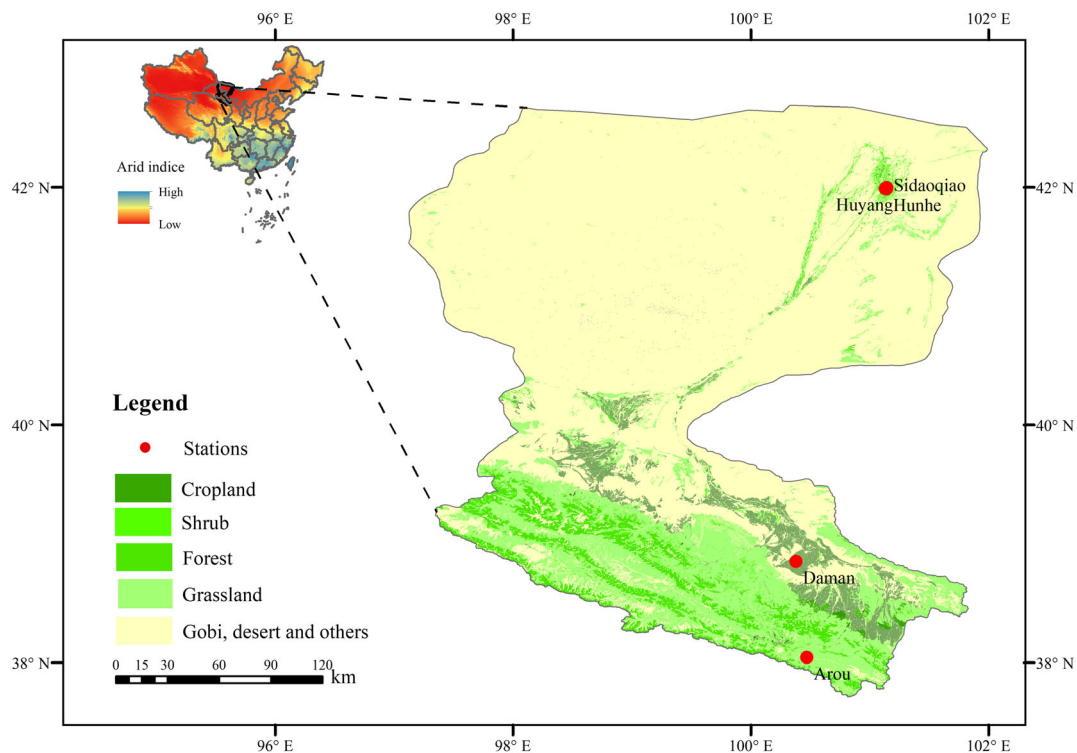


FIGURE 1 Study sites in the Heihe River Basin. Location details and climate characteristics are provided in Table 1

TABLE 1 Locations and climate data of the study sites used in this study

Site	Longitude (°N)	Latitude (°E)	MAT (°C)	MAP (mm)
Arou	38.0473	100.4643	-0.29	444.7
Daman	38.85551	100.3722	6.93	135.7
Sidaoqiao	42.0012	101.1374	10.06	37.13
Hunhe	41.9903	101.1335	10.04	35.53
Huyang	41.9928	101.1236	10.33	26.00

Note: MAT, mean annual temperature; MAP, mean annual precipitation.

Eco-hydrological observations include greenhouse gas fluxes and meteorological measurements using the eddy covariance (EC) towers in the Heihe River Basin (Li et al., 2013).

We used field observations from five stations, covering lower to upper reaches. These stations were installed along the climatic gradient at Huyang, Hunhe, Sidaoqiao, Daman and Arou within the Heihe River Basin (Figure 1 and Table 1). Fluxes data of CO₂, water, and heat were automatically collected by an open-path, infrared gas analyser (Li-7500, LiCor Inc., USA) and a three-dimensional sonic anemometer (CSAT3, Campbell Inc., USA) (Liu et al., 2011). Five automatic weather stations (AWS) were established to measure air temperatures and humidity (HMP45C, Vaisala), solar radiation (PSP, Eppley and PIP, Eppley), as well as soil temperature (HFP01, Hukseflu), soil heat flux (HFT3, Campbell) and SMC (CS616, Campbell Inc., USA) from 4-cm soil layers. Data was recorded by a data logger (CR5000, Campbell Scientific Inc.) at a frequency of 10 Hz for all the stations.

VPD and SMC are coupled at monthly and annual scales but tend to be decoupled at a daily scale (Liu, Gudmundsson, et al., 2020; Novick et al., 2016). In this study, half-hour data was used to separate the effects of VPD and SMC. Half-hour data with high quality of interpolation was selected for analysis including observations in 2013 for Arou, 2015 for Huyang, 2016 for Daman and Sidaoqiao, and 2017 for Hunhe. In our analyses, we only used data collected from July because July is the peak growing season and the variation magnitude of environmental factors are relatively small. In addition, we filtered the data and only included the ones with PAR ranging between 500 and 1500 μmol/m² to eliminate periods with strong solar radiation, which constrained LUE (Cleverly et al., 2020; Novick et al., 2016). The SMC constraint on LUE was indicated by comparing the effect of SMC under different water conditions.

2.2 | Flux data quality control, filling and partitioning

Firstly, 10 Hz data of heat and CO₂ flux were processed by EdiRe software (<https://www.campbellsci.com/>) to obtain half-hour data. Processing included despiking, coordinate rotation, time lag correction, frequency response correction and Webb–Pearman–Leuning calibration (WPL) (Yu et al., 2006). Secondly, we eliminated the CO₂, water and heat flux data with low quality. Considering steady state and integral turbulence, the flux data of CO₂, water and energy was

classified by different quality level according to quality assessment and control (QA/QC) (Isaac et al., 2017), and we only selected flux data with high quality. Data would be screened if there were precipitation and if the equipment malfunctioned. The data measured at low value of u^* were also excluded. The threshold was 0.1 m/s in Arou, 0.2 m/s in Daman, 0.1 m/s in Hunhe and 0.15 m/s in Huyang (Wang et al., 2018). After removing errors and low-quality data, we used the non-linear function methods of Michaelis–Menten (Equation 1) (Falge et al., 2001a) and Lloyd–Taylor (Equation 2) (Ahmed et al., 2017) to interpolate missing values (Biederman et al., 2017). The missing values were interpolated by nonlinear fitting, from which α (initial quantum yield), P_{max} (maximum photosynthetic rate), a , and b were derived. We calculated the R^2 of the fitting to assess the quality of interpolation (Falge et al., 2001b). R^2 ranged from 0.58 to 0.76 (Table S1). Thus, the interpolation quality was adequate for further analysis.

$$NEE = -\frac{\alpha \times PAR \times P_{max}}{\alpha \times PAR + P_{max}} \quad (1)$$

where NEE , α , PAR , P_{max} represent net ecosystem exchange, initial quantum yield, photosynthetically active radiation, and the maximum photosynthetic rate, respectively;

$$Reco = a \times \exp^{bT_s} \quad (2)$$

where a and b are constants, and $Reco$ and T_s represent ecosystem respiration and the soil temperature at a depth 5 cm, respectively. We then calculated GPP following Fei et al. (2019):

$$GPP = Reco - NEE \quad (3)$$

There are different definitions of LUE (either the ratio of GPP to absorption of photosynthetically active radiation (APAR) or the ratio of GPP to photosynthetically active radiation (PAR)). In this study, ecological LUE was used to represent ecosystem LUE, which was defined as follows (Fei et al., 2019):

$$LUE = \frac{GPP}{PAR} \quad (4)$$

VPD was calculated with the following equation (Venturini et al., 2011):

$$VPD = 0.61078 \times e^{\frac{117.27 \times Ta}{Ta + 237.5}} \times (1 - RH) \quad (5)$$

where *Ta* and *RH* represents air temperature and relative humidity, respectively.

2.3 | Analysis methods

We analysed the effect of *SMC* on *LUE* with different soil moisture conditions in four sites as well as one site with significantly variable soil moisture dynamics. We used two methods aiming to strengthen the robustness of our analyses of the impact of *VPD* and *SMC* on *LUE*. We firstly divided *VPD* data of each site by method of data box (Liu, Gudmundsson, et al., 2020). The *VPD* data was divided into 10 to 15 bins according to the range of *VPD* in different sites. *SMC* of four sites ranged from 30% to 40% at Daman, 20% to 30% at Sidaoqiao, 10% to 20% at Hunhe and 0% to 10% at Huyang. We used the natural

range of *SMC* at each of the four sites and used the four sites together to evaluate the effect of *SMC* constraint on *LUE* under different soil moisture conditions. Arou was a relatively moist site with *SMC* ranging from 10% to 50%. As such, we selected Arou as a single site to analyse the *SMC* constraint on *LUE* under different soil moisture conditions. The data of *SMC* in Arou were similarly divided into bins of 40%–50%, 30%–40%, 20%–30% and 10%–20%.

The piecewise linear regression was used to analyse the relationships between *VPD* and *LUE*. Piecewise linear regression firstly examined whether a break point (threshold) existed in the regression line. Then a linear regression was fitted below and above the threshold. We further examined how the effect of *SMC* on *LUE* varied under different *SMC*. The Pearson's *r* between *LUE* and *SMC* was also calculated. We analysed the changes of Pearson's *r* with increasing *VPD* to evaluate the interaction of *VPD*, *SMC* and *LUE*.

We identified the maximum *LUE* value when *VPD* is near zero without *VPD* constraint. We also identified the *LUE* value when *VPD*

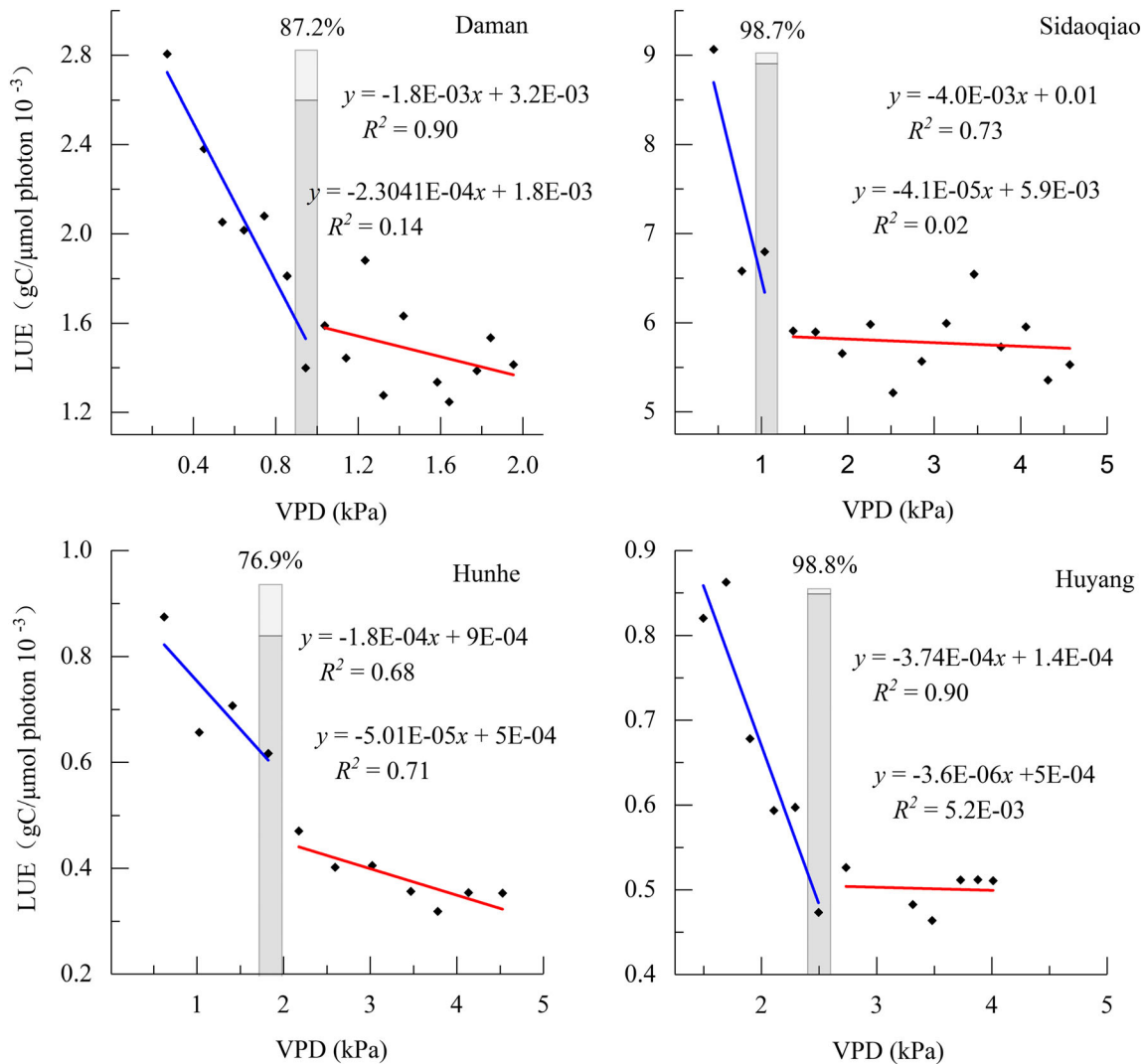


FIGURE 2 Responses of light-use efficiency (*LUE*) to rising vapour–pressure deficit (*VPD*). Blue lines represent the relationship below the threshold; red lines represent that above the threshold. Dark and light grey bars represent the slopes of the relationship below and above the threshold. The percentages represent the decrease in the slope below and above the threshold

was near the threshold, exceeding which the *LUE* would not significantly decrease. This *LUE* value was considered the minimum *LUE* value constrained by *VPD*. The difference of maximum and minimum *LUE* constrained by *VPD* was considered the reduction of *LUE* (*fLUE*) constrained by *VPD*. Therefore, we consider the remaining *LUE* (*rLUE*) was not significantly affected by *VPD*. All statistical analyses were performed in Python (<https://www.python.org/>), and graphs were made using Origin 2017 (<https://www.originlab.com/>).

3 | RESULTS

3.1 | Threshold for the constraint of *LUE* by *VPD*

The relationship between *VPD* and *LUE* showed a threshold at all sites (Figure 2). When *VPD* was below the threshold, *LUE* decreased rapidly, with a decreasing ratio of 2.0×10^{-4} to 2.2×10^{-3} $\text{gC } \mu\text{mol photon kPa}^{-1}$, but when *VPD* was above the threshold, the decreasing ratio reduced to between 4.0×10^{-6} and 3.0×10^{-4} $\text{gC } \mu\text{mol photon kPa}^{-1}$. This represents a decrease of 86.4% to 98.0% compared with the value below the threshold; that is, the constraint effect was small when *VPD* exceeds the threshold. Further, a threshold also existed under different *SMC* conditions at one single site (Figure 3) for all four ranges of *SMC*. When *VPD* exceeds the threshold, the slope of the *VPD*-*LUE* relationship decreased by 77.3% to 93.3%.

3.2 | Effect of *SMC* on the threshold

We analysed changes in the *VPD* threshold in response to changes in *SMC* to evaluate the relative impacts of *SMC* on *LUE* (Figure 3). The

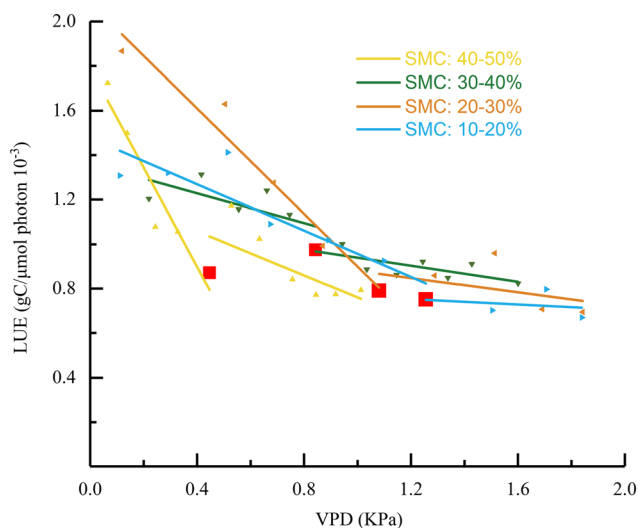


FIGURE 3 Responses of light-use efficiency (*LUE*) to rising vapour-pressure deficit (*VPD*) under different soil water conditions at Arou. Half-hour data of soil moisture content (*SMC*) in Arou was divided into different water conditions (40%–50%, 30%–40%, 20%–30% and 10%–20%). The red points represent the thresholds identified by piecewise linear regression

threshold differed significantly between the different *SMC* regimes, with *VPD* values of 0.9 kPa at *SMC* ranging from 30% to 40%, 1.0 kPa at *SMC* ranging from 20% to 30%, and 1.8 kPa at *SMC* ranging from 10% to 20%, 2.5 kPa at *SMC* ranging from 0% to 10%. That is, the *VPD* threshold increased with decreasing *SMC*.

Moreover, the reduction of *LUE* caused by *VPD* alone (*fLUE*) also changed with *SMC* (Figure 4). *fLUE* increased with increasing *SMC*, with *fLUE* of 49.4% to 50.1% in the moister region (Daman and Sidaoqiao) and only 17.3% to 19.1% in the more arid region (Hunhe and Huyang). In contrast, *rLUE* increased with decreasing *SMC*, with the largest values in the two drier regions.

3.3 | Interactions among *VPD*, *SMC* and *LUE*

We calculated Pearson's *r* between *SMC* and *LUE* and analysed how *r* changed with increasing *VPD* to clarify the interactions among *VPD*, *SMC* and *LUE* (Figure 5). The correlation weakened with increasing *VPD* until it reached a threshold, then increased thereafter. When *VPD* was below the threshold, the absolute value of *r* decreased, sometimes to 0, with increasing *VPD*. Therefore, the effect of *SMC* on *LUE* decreased with increasing *VPD* when *VPD* was below the threshold. However, when *VPD* exceeds a threshold, the absolute value of *r* increased with increasing *VPD*, indicating that the importance of *SMC* increased with decreasing *VPD*.

The soil heat fluxes and soil temperature also showed pronounced changes in response to *VPD* (Figure 6). With increasing *VPD*, all soil heat fluxes and soil temperature increased abruptly, indicating

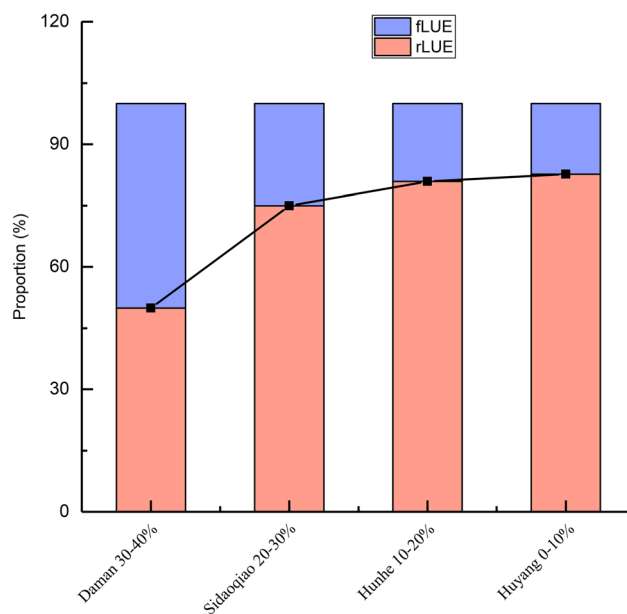


FIGURE 4 The reduction of light-use efficiency (*LUE*) when vapour-pressure deficit (*VPD*) increases from its minimum value to the threshold at different sites with different dominant soil moisture content (*SMC*). *fLUE* and *rLUE* represent reduction of *LUE* and the remaining *LUE*. Black line represent how *fLUE* and *rLUE* changed with decreasing dominant *SMC* conditions

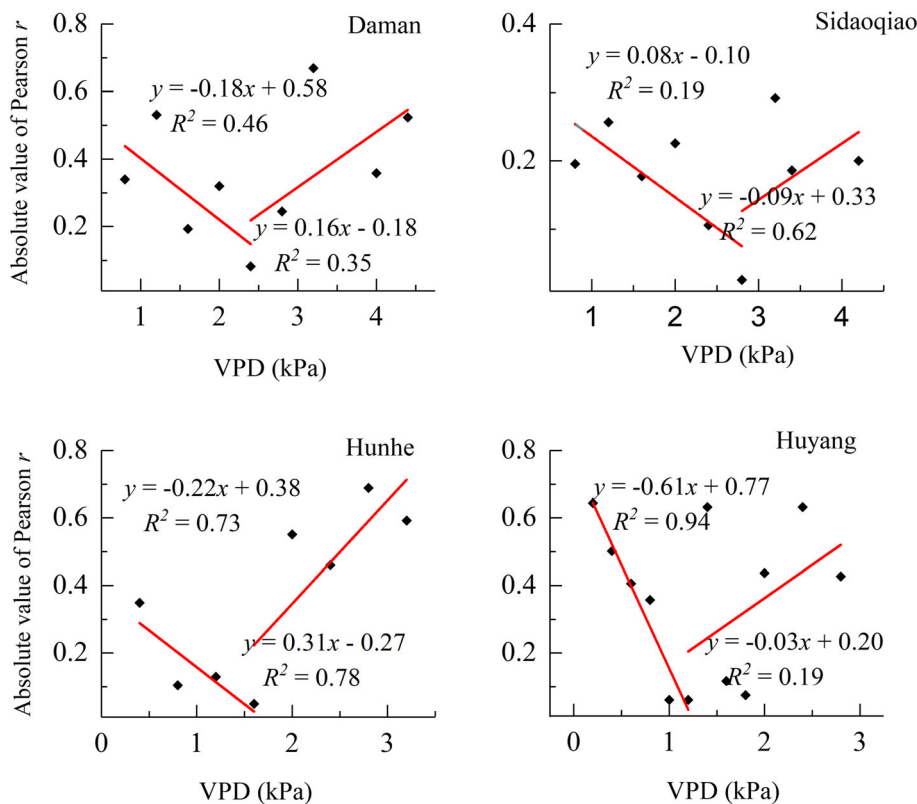


FIGURE 5 Response of the absolute value of Pearson's r between soil moisture content (SMC) and light-use efficiency (LUE) with rising vapour-pressure deficit (VPD). Dark point represents the absolute value of r calculated in each data box. Red lines represent fitting line between $|r|$ and VPD

the existence of a threshold, whereas AET decreased with increasing VPD (Figure S1).

4 | DISCUSSION

Previous studies have emphasized the constraint of LUE by either VPD (Yuan et al., 2019) or SMC (Stocker et al., 2018), but our results demonstrate that both factors play essential roles in how water stress limits LUE and that their relative importance differs at different levels of water stress.

4.1 | Role of VPD in constraining LUE

The rate of VPD induced LUE reduction decreased greatly, by 86.4% to 98.0%, when VPD crossed a threshold, which existed both for multiple sites with different water moisture regimes and for one site with different water conditions (Figure 4). Moreover, soil heat fluxes and temperature increased abruptly with rising VPD, whereas AET decreased simultaneously (Figure S1). According to an empirical model of the relationship between VPD and LUE (Oren et al., 1999), the rate of stomatal decrease would slow when VPD increased beyond a large value (Novick et al., 2016). Hence, the rate of LUE decrease would decrease significantly above a threshold (Fletcher et al., 2007). With the reduction of stomatal conductance, AET and the cooling effect from this water loss would decrease. As a result, soil temperature increased when VPD increases above a threshold (Forzieri

et al., 2020). The abrupt change of soil heat flux and AET further supported the existence of a threshold, indicating that the exchanges of water and heat between soil, plant and atmosphere also changed near the threshold. The strength of the correlation ($|r|$) between SMC and LUE decreased greatly with rising VPD when VPD was below the threshold but increased with rising VPD when VPD exceeded the threshold (Figure 5). The variation of Pearson's r indicates that SMC constraint on LUE decreased with rising VPD below the threshold, which resulted from initial control of VPD on AET and LUE. However, SMC constraint on LUE increased with rising VPD when VPD was above the threshold because of vegetation water stress and the decrease of VPD constraint on LUE. Therefore, the variation of Pearson's r could also support the dynamic VPD constraint on LUE.

Our results indicate different linear relationships between VPD and LUE below and above the threshold. The rate of change in LUE above the threshold was less than 25% of the rate below the threshold, and as low as 2% of that rate. The strength of the correlation ($|r|$) between SMC and LUE decreased greatly with rising VPD below the threshold. Therefore, VPD had the strongest effect on LUE when VPD was below the threshold. The effect of VPD on stomatal conductance and LUE was greater when VPD was below the threshold, which agrees with an empirical formula developed for stomatal conductance (Oren et al., 1999). On the other hand, the constraint of LUE by VPD would be overestimated if all high VPD levels were used to represent water limitation, as there is no continuous significant decrease of LUE when VPD exceeds a threshold. The overestimation of VPD constraint was also present in a previous yield loss simulation, in which the crop yield reduction caused by VPD constraint of LUE was overestimated

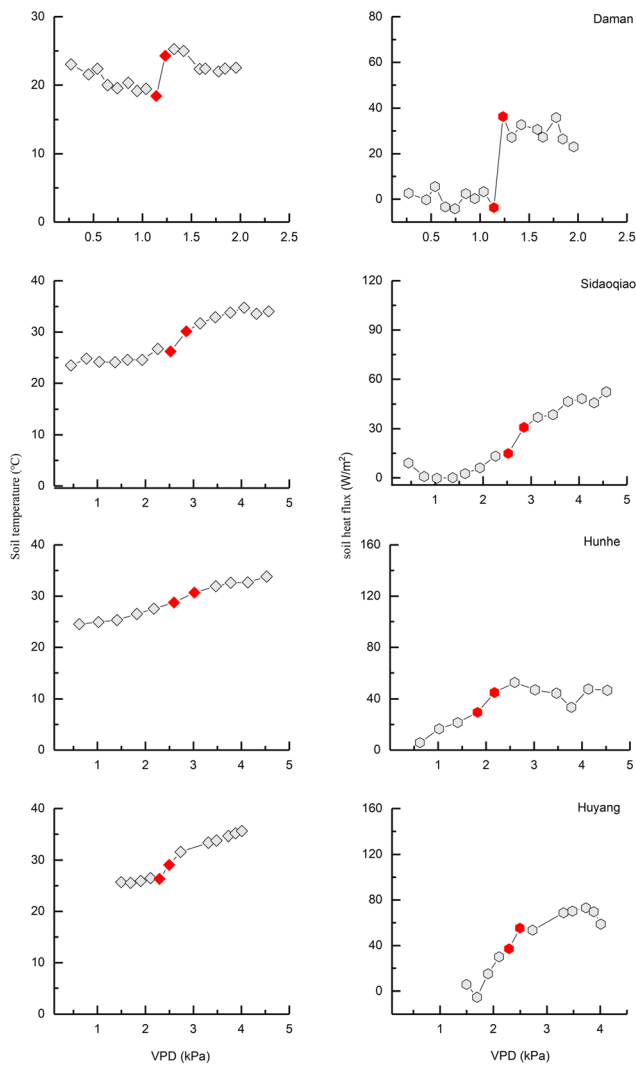


FIGURE 6 The responses of soil temperature and soil heat flux to rising vapour–pressure deficit (VPD)

by a factor of two, mainly as a result of the failure to capture the slower decrease of *LUE* when *VPD* is above a threshold (Rigden et al., 2020). *VPD* limits photosynthesis by decreasing stomatal conductance, but this limitation will not significantly reduce photosynthesis after a high *VPD* is reached (Grossiord et al., 2020). Thus, reduction of *LUE* caused by *VPD* constraint decreases above the threshold.

4.2 | Role of *SMC* in constraint of *LUE*

The reduction of *LUE* decreased greatly with decreasing *SMC*, which also indicates a difference in the constraint of *LUE* by *SMC* and *VPD*. The relationship between *SMC* and *LUE* showed a turning point with rising *VPD*. The absolute value of *r* between *SMC* and *LUE* first decreased with increasing *VPD* and then increased above the threshold. Pearson's *r* between *SMC* and *LUE* could indicate the strength of *SMC* effect on *LUE*. Thus, the relative importance of *SMC* increased and the effect of *SMC* on *LUE* was stronger when *VPD* was above the

threshold. Initially, rising *VPD* would significantly decrease *AET* by reducing stomatal conductance when *VPD* was below the threshold (Novick et al., 2016). *AET* and heat exchange therefore changed with increasing *VPD* (Figure 6, Figure S1). Consequently, the consumption of *SMC* initially decreases owing to decreasing *AET* (Anderegg & Venturas, 2020), which would weaken the relationship between *SMC* and *LUE*. However, with *VPD* continuing to increase, available water would decrease, leading to increasing water stress (Grossiord et al., 2020). Therefore, *SMC*, which represents the direct source of water available to the plant, would be essential for maintenance of photosynthesis and other processes as *VPD* continues to increase (Trugman et al., 2018). Under these circumstances, *SMC* becomes vital to maintaining photosynthesis. In the two driest regions (Hunhe and Huyang), the lower threshold for *VPD* (based on $|r|$ in Figure 5) also supports this hypothesis. The lower threshold indicated that *SMC* was more important at Hunhe and Huyang owing to their lower *SMC*, which made photosynthesis more depend on the direct water resource represented by *SMC*.

With *SMC* decreasing, the threshold of *VPD* constraint for *LUE* become larger, further reduction of *LUE* created by *VPD* decreased, with a reduction of *VPD* contribution to the total constraint to 49.4% to 50.1% in moister region and a reduction of *VPD* constraint to only 17.3% to 19.1% in more arid region (Figure 4). Therefore, *VPD* constraint of *LUE* was more important in moister regions, whereas *SMC* was more important in more arid regions. Hence, the different importance of *VPD* and *SMC* in limiting *LUE* may have resulted from different water regimes. Reduction of *LUE* by *VPD* constraint was larger in more humid regions, thus, *VPD* would play the dominant role in limiting *LUE* in such regions (Novick et al., 2016; Yuan et al., 2019). Furthermore, the reduction of *LUE* by *SMC* constraint was larger in drier regions, *SMC* would play the dominant role in limiting *LUE* in such regions (Liu, Gudmundsson, et al., 2020; Stocker et al., 2018). A previous study also suggested that both *VPD* and *SMC* are important in the constraint of *LUE* (Rigden et al., 2020). *SMC* determined the range of the reduction, but the constraint effect of *VPD* was stronger than *SMC* when *VPD* was below the threshold. Consequently, considering only *VPD* or *SMC* would result in considerable errors in simulating photosynthesis (Rigden et al., 2020).

4.3 | Implications for carbon cycle simulation

The relative constraints caused by *VPD* and *SMC* varied with decreasing *SMC* (Figure 4), indicating that variation of *SMC* would change the relationships among *VPD*, *SMC* and *LUE*. These changes would regulate the vegetation responses to water stress, thereby changing photosynthesis and the carbon cycle in arid and semi-arid regions (Rogers et al., 2017; Stocker et al., 2019). The precipitation in arid regions fluctuates greatly, causing high variation of *SMC*. This exacerbates the impacts of water stress because photosynthesis of plants in arid regions can be more sensitive to changes in water availability (Gonsamo et al., 2019). Consequently, the relationships among *VPD*, *SMC* and *LUE* will change frequently in response to a large variation of

SMC (Stocker et al., 2019). This will lead to high uncertainty in simulation of the carbon cycle in arid ecosystems. Specifically, as water conditions change, the threshold and reduction for VPD constraint of LUE will change, but it is essential to account for these changes to reduce the uncertainty in simulations of the carbon cycle in arid regions (Trugman et al., 2018; Zhang et al., 2018). We analysed how LUE changed with different VPD and SMC in five sites. However, biotic processes and characters are critical for vegetation photosynthesis. LUE would significantly vary with vegetation type, indicating that vegetation type significantly affects LUE (Fei et al., 2019). For example, LUE in cropland was different from grassland and forest, which resulted from management practices (Allen et al., 2005).

5 | CONCLUSION

Our study revealed that both VPD and SMC played important roles in how water limitations (i.e., an imbalance between water demand, represented by VPD, and supply, represented by SMC) constrained LUE. We found clear evidence for a threshold for constraint of LUE by VPD. The rate of LUE reduction at VPD above the threshold was only 3.6% to 23.1% of that below the threshold. Furthermore, the threshold and the magnitude of the reduction of LUE above that threshold were affected by SMC. The VPD threshold increased with decreasing SMC. With decreasing SMC at different sites, the reduction of VPD constraint decreased, with VPD contribution of 49.4% to 50.1% of the total at moister sites, but decreasing to 17.3% to 19.1% in more arid regions. Consequently, VPD had a more important effect on LUE in moister regions, whereas SMC became more important in more arid regions. The interactions among VPD, SMC and LUE and soil heat flux also support the relative strengths of the constraint of LUE created by VPD and SMC. The strength of the correlation between SMC and LUE decreased below the threshold, then increased again above it, whereas soil temperature and heat flux increased with increasing VPD, which resulted in the changes in the relative roles of VPD and SMC.

This study was conducted in arid and semi-arid region to analyse the constraint process of VPD and SMC, aiming to quantify the relative role of VPD and SMC in water limitation on LUE. However, the constraint process in moisture region may differ from that in arid and semi-arid region. To illustrate the water limitation process, therefore, mechanistic understanding of constraint of VPD and SMC are needed in moist region to clarify the interaction process among VPD, SMC and LUE, which may differ in moist regions and drylands.

ACKNOWLEDGEMENTS

This work was supported by National Natural Science Foundation of China (41991230), “the Fundamental Research Funds for the Central Universities, and Bayannur Ecological Governance and Green Development Academician Expert Workstation (YSZ2018-1).” The data in this study are obtained from Heihe Watershed Allied Telemetry Experimental Research (HiWATER) field campaigns, and we appreciate all people contribute to this project. We also thank the editors and

reviewers for improving this manuscript on this work. A special thanks to Dongxing Wu for method of interpolation.

DATA AVAILABILITY STATEMENT

The authors confirm that the data supporting the findings of this study are available from dataset of Heihe Watershed Allied Telemetry Experimental Research (HiWATER) Monitoring & Big Data Center for Three Poles.

ORCID

Dexin Gao  <https://orcid.org/0000-0002-1934-9689>

REFERENCES

- Ahmed, M., Else, B., Eklundh, L., Ardö, J., & Seaquist, J. (2017). Dynamic response of ndvi to soil moisture variations during different hydrological regimes in the sahel region. *International Journal of Remote Sensing*, 38, 5408–5429. <https://doi.org/10.1080/01431161.2017.1339920>
- Allen, C. B., Will, R. E., McGarvey, R. C., Coyle, D. R., & Coleman, M. D. (2005). Radiation-use efficiency and gas exchange responses to water and nutrient availability in irrigated and fertilized stands of sweetgum and sycamore. *Tree Physiology*, 25, 191–200. <https://doi.org/10.1093/treephys/25.2.191>
- Anderegg, W. R. L., & Venturas, M. D. (2020). Plant hydraulics play a critical role in Earth system fluxes. *New Phytologist*, 226, 1535–1538. <https://doi.org/10.1111/nph.16548>
- Bartlett, M. K., Klein, T., Jansen, S., Choat, B., & Sack, L. (2016). The correlations and sequence of plant stomatal, hydraulic, and wilting responses to drought. *Proceedings of the National Academy of Sciences of the United States of America*, 113, 13098–13103. <https://doi.org/10.1073/pnas.1604088113>
- Biederman, J. A., Scott, R. L., Bell, T. W., Bowling, D. R., Dore, S., Garatuza-Payan, J., Kolb, T. E., Krishnan, P., Krofcheck, D. J., Litvak, M. E., Maurer, G. E., Meyers, T. P., Oechel, W. C., Papuga, S. A., Ponce-Campos, G. E., Rodriguez, J. C., Smith, W. K., Vargas, R., Watts, C. J., ... Goulden, M. L. (2017). CO₂ exchange and evapotranspiration across dryland ecosystems of southwestern North America. *Global Change Biology*, 23, 4204–4221. <https://doi.org/10.1111/gcb.13686>
- Cleverly, J., Vote, C., Isaac, P., Ewenz, C., Harahap, M., Beringer, J., Campbell, D. I., Daly, E., Eamus, D., He, L., Hunt, J., Grace, P., Hutley, L. B., Laubach, J., McCaskill, M., Rowlings, D., Rutledge Jonker, S., Schipper, L. A., Schroder, I., ... Grover, S. P. P. (2020). Carbon, water and energy fluxes in agricultural systems of Australia and New Zealand. *Agricultural and Forest Meteorology*, 287, 107934. <https://doi.org/10.1016/j.agrformet.2020.107934>
- Falge, E., Baldocchi, D., Olson, R., Anthoni, P., Aubinet, M., Bernhofer, C., Burba, G., Ceulemans, R., Clement, R., Dolman, H., Granier, A., Gross, P., Grünwald, T., Hollinger, D., Jensen, N. O., Katul, G., Keronen, P., Kowalski, A., Lai, C. T., ... Wofsy, S. (2001a). Gap filling strategies for defensible annual sums of net ecosystem exchange. *Agricultural and Forest Meteorology*, 107, 43–69. [https://doi.org/10.1016/S0168-1923\(00\)00225-2](https://doi.org/10.1016/S0168-1923(00)00225-2)
- Falge, E., Baldocchi, D., Olson, R., Anthoni, P., Aubinet, M., Bernhofer, C., Burba, G., Ceulemans, R., Clement, R., Dolman, H., Granier, A., Gross, P., Grünwald, T., Hollinger, D., Jensen, N.-O., Katul, G., Keronen, P., Kowalski, A., Ta Lai, C., ... Wofsy, S. (2001b). Gap filling strategies for long term energy flux data sets. *Agricultural and Forest Meteorology*, 107(1), 71–77. [https://doi.org/10.1016/s0168-1923\(00\)00235-5](https://doi.org/10.1016/s0168-1923(00)00235-5)
- Fei, X. H., Song, Q. H., Zhang, Y. P., Yu, G. R., Zhang, L. M., Sha, L. Q., Liu, Y. T., Xu, K., Chen, H., Wu, C. S., Chen, A. G., Zhang, S. B., Liu, W. W., Huang, H., Deng, Y., Qin, H. L., Li, P. G., & Grace, J. (2019). Patterns and Controls of Light Use Efficiency in Four Contrasting

- Forest Ecosystems in Yunnan, Southwest China. *Journal of Geophysical Research: Biogeosciences*, 124, 293–311. <https://doi.org/10.1029/2018JG004487>
- Fletcher, A. L., Sinclair, T. R., & Allen, L. H. (2007). Transpiration responses to vapor pressure deficit in well watered “slow-wilting” and commercial soybean. *Environmental and Experimental Botany*, 61, 145–151. <https://doi.org/10.1016/j.envexpbot.2007.05.004>
- Forzieri, G., Miralles, D. G., Ciais, P., Alkama, R., Ryu, Y., Duveiller, G., Zhang, K., Robertson, E., Kautz, M., Martens, B., Jiang, C., Arneeth, A., Georgievski, G., Li, W., Ceccherini, G., Anthoni, P., Lawrence, P., Wiltshire, A., Pongratz, J., ... Cescatti, A. (2020). Increased control of vegetation on global terrestrial energy fluxes. *Nature Climate Change*, 10, 356–362. <https://doi.org/10.1038/s41558-020-0717-0>
- Gonsamo, A., Chen, J. M., He, L., Sun, Y., Rogers, C., & Liu, J. (2019). Exploring SMAP and OCO-2 observations to monitor soil moisture control on photosynthetic activity of global drylands and croplands. *Remote Sensing of Environment*, 232, 111314. <https://doi.org/10.1016/j.rse.2019.111314>
- Grossiord, C., Buckley, T. N., Cernusak, L. A., Novick, K. A., Poulter, B., Siegwolf, R. T. W., Sperry, J. S., & McDowell, N. G. (2020). Plant responses to rising vapor pressure deficit. *New Phytologist*, 226, 1550–1566. <https://doi.org/10.1111/nph.16485>
- Hsiao, J., Swann, A. L. S., & Kim, S.-H. (2019). Maize yield under a changing climate: The hidden role of vapor pressure deficit. *Agricultural and Forest Meteorology*, 279, 107692. <https://doi.org/10.1016/j.agrformet.2019.107692>
- Isaac, P., Cleverly, J., McHugh, I., Van Gorsel, E., Ewenz, C., & Beringer, J. (2017). OzFlux data: Network integration from collection to curation. *Biogeosciences*, 14, 2903–2928. <https://doi.org/10.5194/bg-14-2903-2017>
- Lanning, M., Wang, L., Scanlon, T. M., Vadeboncoeur, M. A., Adams, M. B., Epstein, H. E., & Druckenbrod, D. (2019). Intensified vegetation water use under acid deposition. *Science Advances*, 5, 1–10. <https://doi.org/10.1126/sciadv.aav5168>
- Li, X., Cheng, G., Liu, S., Xiao, Q., Ma, M., Jin, R., Che, T., Liu, Q., Wang, W., Qi, Y., Wen, J., Li, H., Zhu, G., Guo, J., Ran, Y., Wang, S., Zhu, Z., Zhou, J., Hu, X., & Xu, Z. (2013). Heihe watershed allied telemetry experimental research (HiWater) scientific objectives and experimental design. *Bulletin of the American Meteorological Society*, 94, 1145–1160. <https://doi.org/10.1175/BAMS-D-12-00154.1>
- Liu, L., Gudmundsson, L., Hauser, M., Qin, D., Li, S., & Seneviratne, S. I. (2020). Soil moisture dominates dryness stress on ecosystem production globally. *Nature Communications*, 11, 4892. <https://doi.org/10.1038/s41467-020-18631-1>
- Liu, S. M., Xu, Z. W., Wang, W. Z., Jia, Z. Z., Zhu, M. J., Bai, J., & Wang, J. M. (2011). A comparison of eddy-covariance and large aperture scintillometer measurements with respect to the energy balance closure problem. *Hydrology and Earth System Sciences*, 15, 1291–1306. <https://doi.org/10.5194/hess-15-1291-2011>
- Liu, Y., Kumar, M., Katul, G. G., Feng, X., & Konings, A. G. (2020). Plant hydraulics accentuates the effect of atmospheric moisture stress on transpiration. *Nature Climate Change*, 10, 691–695. <https://doi.org/10.1038/s41558-020-0781-5>
- Mccarter, C. P. R., & Price, J. S. (2014). Ecohydrology of Sphagnum moss hummocks: Mechanisms of capitula water supply and simulated effects of evaporation. *Ecohydrology*, 7, 33–44. <https://doi.org/10.1002/eco.1313>
- McDowell, N. G., & Allen, C. D. (2015). Darcy's law predicts widespread forest mortality under climate warming. *Nature Climate Change*, 5, 669–672. <https://doi.org/10.1038/nclimate2641>
- Monteith, J. L., & Moss, C. J. (1977). Climate and the Efficiency of Crop Production in Britain [and Discussion]. *Philosophical Transactions of the Royal Society B: Biological Sciences*, 281, 277–294.
- Novick, K. A., Ficklin, D. L., Stoy, P. C., Williams, C. A., Bohrer, G., Oishi, A. C., Papuga, S. A., Blanken, P. D., Noormets, A., Sulman, B. N., Scott, R. L., Wang, L., & Phillips, R. P. (2016). The increasing importance of atmospheric demand for ecosystem water and carbon fluxes. *Nature Climate Change*, 6, 1023–1027. <https://doi.org/10.1038/nclimate3114>
- Oren, R., Sperry, J. S., Katul, G. G., Pataki, D. E., Ewers, B. E., Phillips, N., & Schäfer, K. V. R. (1999). Survey and synthesis of intra- and interspecific variation in stomatal sensitivity to vapour pressure deficit. *Plant, Cell and Environment*, 22, 1515–1526. <https://doi.org/10.1046/j.1365-3040.1999.00513.x>
- Rigden, A. J., Mueller, N. D., Holbrook, N. M., Pillai, N., & Huybers, P. (2020). Combined influence of soil moisture and atmospheric evaporative demand is important for accurately predicting US maize yields. *Nature Food*, 1, 127–133. <https://doi.org/10.1038/s43016-020-0028-7>
- Rogers, A., Medlyn, B. E., Dukes, J. S., Bonan, G., von Caemmerer, S., Dietze, M. C., Kattge, J., Leakey, A. D. B., Mercado, L. M., Niinemets, Ü., Prentice, I. C., Serbin, S. P., Sitch, S., Way, D. A., & Zaehle, S. (2017). A roadmap for improving the representation of photosynthesis in Earth system models. *New Phytologist*, 213, 22–42. <https://doi.org/10.1111/nph.14283>
- Seneviratne, S. I., Corti, T., Davin, E. L., Hirschi, M., Jaeger, E. B., Lehner, I., Orlowsky, B., & Teuling, A. J. (2010). Investigating soil moisture-climate interactions in a changing climate: A review. *Earth-Science Reviews*, 99, 125–161. <https://doi.org/10.1016/j.earscirev.2010.02.004>
- Song, C. (2019). Preface to the special issue on the ecological-hydrological processes in the Heihe River Basin: Integrated research on observation, modeling and data analysis. *Journal of Geographical Sciences*, 29, 1437–1440. <https://doi.org/10.1007/s11442-019-1680-4>
- Stocker, B. D., Zscheischler, J., Keenan, T. F., Prentice, I. C., Peñuelas, J., & Seneviratne, S. I. (2018). Quantifying soil moisture impacts on light use efficiency across biomes. *New Phytologist*, 218, 1430–1449. <https://doi.org/10.1111/nph.15123>
- Stocker, B. D., Zscheischler, J., Keenan, T. F., Prentice, I. C., Seneviratne, S. I., & Peñuelas, J. (2019). Drought impacts on terrestrial primary production underestimated by satellite monitoring. *Nature Geoscience*, 12, 264–270. <https://doi.org/10.1038/s41561-019-0318-6>
- Stocker, T.F., Qin, D., Plattner, G.K., Alexander, L. V., Allen, S.K., Bindoff, N.L., Bréon, F.M., Church, J.A., Cubasch, U., Emori, S., 2013. IPCC, 2013: Technical Summary. In: Climate Change 2013: The Physical Science Basis. Contribution of Working Group I to the Fifth Assessment Report of the Intergovernmental Panel on Climate Change [Stocker, T.F., D. Qin, G.-K. Plattner, M. Tignor, S.K. All.
- Taylor, N., Price, J., & Strack, M. (2016). Hydrological controls on productivity of regenerating Sphagnum in a cutover peatland. *Ecohydrology*, 9, 1017–1027. <https://doi.org/10.1002/eco.1699>
- Trugman, A. T., Medvigy, D., Mankin, J. S., & Anderegg, W. R. L. (2018). Soil Moisture Stress as a Major Driver of Carbon Cycle Uncertainty. *Geophysical Research Letters*, 45, 6495–6503. <https://doi.org/10.1029/2018GL078131>
- Venturini, V., Rodriguez, L., & Bisht, G. (2011). A comparison among different modified priestley and taylor equations to calculate actual evapotranspiration with MODIS data. *International Journal of Remote Sensing*, 32, 1319–1338. <https://doi.org/10.1080/01431160903547965>
- Wang, H., Li, X., Ma, M., & Geng, L. (2019). Improving estimation of gross primary production in dryland ecosystems by a model-data fusion approach. *Remote Sensing*, 11(3), 225. <https://doi.org/10.3390/rs11030225>
- Wang, M., Wu, J., Lafleur, P. M., Luan, J., Chen, H., & Zhu, X. (2018). Temporal shifts in controls over methane emissions from a boreal bog. *Agricultural and Forest Meteorology*, 262, 120–134. <https://doi.org/10.1016/j.agrformet.2018.07.002>
- Wu, J., Jing, Y., Guan, D., Yang, H., Niu, L., Wang, A., Yuan, F., & Jin, C. (2013). Controls of evapotranspiration during the short dry season in a

- temperate mixed forest in Northeast China. *Ecohydrology*, 6, 775–782. <https://doi.org/10.1002/eco.1299>
- Yu, G. R., Wen, X. F., Sun, X. M., Tanner, B. D., Lee, X., & Chen, J. Y. (2006). Overview of ChinaFLUX and evaluation of its eddy covariance measurement. *Agricultural and Forest Meteorology*, 137, 125–137. <https://doi.org/10.1016/j.agrformet.2006.02.011>
- Yuan, W., Cai, W., Xia, J., Chen, J., Liu, S., Dong, W., Merbold, L., Law, B., Arain, A., Beringer, J., Bernhofer, C., Black, A., Blanken, P. D., Cescatti, A., Chen, Y., Francois, L., Gianelle, D., Janssens, I. A., Jung, M., ... Wohlfahrt, G. (2014). Global comparison of light use efficiency models for simulating terrestrial vegetation gross primary production based on the LaThuile database. *Agricultural and Forest Meteorology*, 192–193, 108–120. <https://doi.org/10.1016/j.agrformet.2014.03.007>
- Yuan, W., Zheng, Y., Piao, S., Ciais, P., Lombardozzi, D., Wang, Y., Ryu, Y., Chen, G., Dong, W., Hu, Z., Jain, A. K., Jiang, C., Kato, E., Li, S., Lienert, S., Liu, S., Nabel, J. E. M. S., Qin, Z., Quine, T., ... Yang, S. (2019). Increased atmospheric vapor pressure deficit reduces global vegetation growth. *Science Advances*, 5, 1–13. <https://doi.org/10.1126/sciadv.aax1396>
- Zhang, X., Dong, K., Xu, K., Zhang, K., Jin, X., Yang, M., Zhang, Y., Wang, X., Han, C., Yu, J., & Li, D. (2018). Barley stripe mosaic virus infection requires PKA-mediated phosphorylation of γ b for suppression of both RNA silencing and the host cell death response. *New Phytologist*, 218, 1570–1585. <https://doi.org/10.1111/nph.15065>

SUPPORTING INFORMATION

Additional supporting information may be found online in the Supporting Information section at the end of this article.

How to cite this article: Gao, D., Wang, S., Li, Z., Wei, F., Chen, P., Song, S., Wang, Y., Wang, L., & Fu, B. (2021). Threshold of vapour–pressure deficit constraint on light use efficiency varied with soil water content. *Ecohydrology*, e2305. <https://doi.org/10.1002/eco.2305>